Microclimate modelling and hygrothermal investigation of freeze-thaw degradation under future climate scenarios

Journal of Physics: Conference Series **2654** (2023) 012146 doi:10.1088/1742-6596/2654/1/012146

Microclimate modelling and hygrothermal investigation of freeze-thaw degradation under future climate scenarios

Jan Mandinec and Pär Johansson

Department of Architecture and Civil Engineering, Chalmers University of Technology, 412 96 Gothenburg, Sweden

jan.mandinec@chalmers.se

Abstract. Future climate scenarios lead to changes in the boundary conditions impacting the service life of building envelopes. This may increase or decrease the risk of degradation caused by e.g., freezing and thawing on brick façades. In this study, the risk of degradation based on individual years is compared for different moisture reference year (MRY) selection methods. Furthermore, two new MRY indices, based on the Frost Decay Exposure Index (FDEI), are proposed to assess future climate scenarios. A brick façade in Gothenburg, Sweden, is used as a case study to investigate the microclimate caused by façade orientation and solar radiation on three different parts of the façade. The risk of damage is compared for climate scenarios A1B and A2 from 1961 to 2100. The microclimate of the façade is modelled to obtain boundary conditions for each part instead of using MRYs as uniform boundary conditions for the whole building. The study demonstrates a 67% difference in risk of degradation between the different parts of the façade. Furthermore, the risk of freeze-thaw degradation reduces in the future. Finally, it is indicated that the basic FDEI index is better at evaluating the severity of exposure compared to its derivatives.

1. Introduction

As an integral part of the building design process, the moisture-safe design aims to ensure that building constructions are resistant to moisture damage and durable in the long term [1]. In the context of designing building envelopes in Nordic countries, one of the main threats to durability is freezing and thawing degradation. To mitigate this risk, the moisture-safe design relies on well-proven solutions or hygrothermal modelling using performance indicators to estimate, e.g., the risk of freeze-thaw degradation. However, the risk may change in the future due to climate change, which can either increase or decrease the risk depending on the location [2]. Such information may provide valuable insight for building owners, managers and designers.

According to the standard EN 15026:2007 [3], an accurate estimation of hygrothermal risks requires hourly climate data at least 10 years long. Alternatively, a reference year, which represents a year with the most severe conditions, can be used to reduce computational time. Most methods for a moisture reference year (MRY) selection were designed to estimate the severity of years concerning mould growth or interstitial condensation. As Vandemeulebroucke [4] highlights, only a handful of methods are suitable for freeze-thaw degradation. As shown in the study, the methods like Freeze-Thaw Cycles based on air temperature (FTC_{air}) [5], Wind-driven Rain from the critical orientation (WDR_{crit}) [6], or Frost Decay Exposure Index (FDEI) [7] already provide reasonable accuracy.

Regardless of the method, the reference year or long series of climate data is usually selected and applied on a whole building envelope uniformly. This means that one set of boundary conditions is

used on all parts of the façades, not considering the local microclimate conditions like overshadowing. However, this may lead to both over- and underestimation of the risk on certain parts of the façade [8]. Therefore, a methodology reflecting the façade's microclimate and evaluating the façade risk of degradation part by part could yield better predictions. Similarly, the MRY selection methods for assessing the severity of freezing and thawing degradation could be developed further to include the façade orientation, its surroundings, and shading from solar radiation by surrounding buildings.

The aim of this study is threefold; 1) to develop the MRY selection methods for freeze-thaw damage, 2) to determine the changes in the severity of freeze-thaw exposure in Gothenburg, Sweden, after 2050, and 3) to quantify the differences in the risk of freeze-thaw degradation on different parts of a façade. The study uses reference years as a base for microclimate modelling of the boundary conditions of the façade for hygrothermal modelling. The microclimate is modelled by the Ladybug toolbox in the Rhino environment [9] and the hygrothermal modelling of the façade is developed as a one-dimensional model in the software WUFI 2D-3 [10]. The case study building has unevenly distributed surface degradation (spalling). The risk of freeze-thaw degradation 20 mm into the brick is investigated on three different parts of the façade. These are areas with high, average, and low incidence solar radiation.

2. Methodology

The first part of the study focuses on improving the Frost Decay Exposure Index (FDEI) by taking site-specific conditions for solar radiation and wind-driven rain into account. Furthermore, the reference year selection is investigated using the performance index for freezing and thawing damage. The second part of the study utilizes the full façade hygrothermal modelling taken from [8], for a case study building in Gothenburg, Sweden. This is used to investigate the performance evaluation of the FDEI index and its derivatives. Furthermore, the procedure is used to address the question of whether differences in freeze-thaw risk of degradation may occur in different parts of the façade.

2.1. FDEI index – adding façade orientation and surroundings

The FDEI index is based on the summation of rainfall intensity that occurs before every transition of the air temperature below 0°C. The summation is performed three times for the periods 48, 72 and 96 hours prior to the transition and averaged together to produce the index. This procedure is taken as a base for creating two modified versions.

The first modification to the index is done by recalculating the rain intensity by the ISO standard [6]. The orientation of the façade, the direction of the wind and its intensity during a rain event, as well as the specifics of the building's surroundings, such as topography, are considered. The equation for the wind-driven rain is:

$$R_{WDR} = \frac{2}{9} * \mathrm{C_R} * \mathrm{C_T} * \mathrm{O} * \mathrm{W} * \cos\theta * U_{10} * R_h^{0.88} \quad (1)$$

where C_r (-) and C_t (-) are the roughness and topography coefficients, O (-) and W (-) are the obstruction and the wall factor, U_{10} (m/s) is the wind speed at 10 m above the ground, θ (-) is the angle of the wind normal to the façade and R_h (mm) is the horizontal rain intensity. The rest of the procedure for FDEI index calculation remains the same as for the original FDEI index. This new version of the index is further called the $\mathrm{FDEI_{wdr}}$ index.

2.2. FDEI index – adding solar radiation

The second index introduced in this paper is created by calculating a weighted average of the $\mathrm{FDEI_{wdr}}$ index and solar radiation, using the average solar radiation values for the corresponding winter period (SR_{winter}). Based on the previous findings [8], [11], wind-driven rain has a significantly higher impact on the final risk of freeze-thaw degradation compared to solar radiation. Therefore, the weights

w_{WDR} = 0.8 for wind-driven rain and w_{solar} = 0.2 for solar radiation are given. The $FDEI_{wdr+solar}$ index is defined by

$$FDEI_{WDR+solar} = \frac{FDEI_{WDR} * w_{WDR} + (1 - SR_{winter} * w_{solar})}{w_{WDR} + w_{solar}} \quad (2)$$

The min-max normalization approach, as defined in Eq. 3, is utilized on $FDEI_{wdr}$ and SR_{winter} prior to the calculation. This is to ensure the scalability between the two variables. Eq. 3 illustrates the calculation of z, which is a normalized value of x. Furthermore, min and max are the observed minimum and maximum values within the dataset.

$$z = \frac{x - \min(x)}{\max(x) - \min(x)} \quad (3)$$

2.3. Evaluation using full-façade modelling

The aim is to evaluate the FDEI indices and the risk of freeze-thaw degradation on different parts of a façade, using the full façade modelling as proposed in [8].

The full façade hygrothermal modelling is performed in two parts. First, microclimate modelling is used to determine boundary conditions over a façade surface. This includes estimations of solar radiation and long-wave counter radiation for various parts of the façade, considering surrounding buildings. This is done using the Ladybug toolbox in the Rhino environment. The methodology allows the wind-driven rain and wind speeds across the façade to be defined either semi-empirically or numerically, using Computational Fluid Dynamics (CFD) simulations. In the second part, a one-dimensional WUFI model is developed for each computational cell and the risk of freeze-thaw degradation is estimated by the means of Freeze-Thaw Degradation Risk (FTDR) index [12]. The points in which the risks are evaluated may be chosen freely based on the evaluation needs.

The effectiveness of the FDEI indices is evaluated by the FTDR index. Two reference years based on the $FTDR_{WDR+solar}$ index for the period before and after 2050 are selected. A ratio based on differences in the FTDR index between the given years is calculated. This is subsequently compared to ratios estimated based on FDEI indices to determine the best MRY selection method. The year 2050 was selected as a dividing point for the study to contrast the severity of years from both halves of the 21st century.

Figure 1. *The object of the case study, the facade of a 60-year-old residential building in Gothenburg,*

Figure 2. *The façade's closest surroundings*

3. Case study

The methodology is applied on a façade of a 60-year-old residential building located in Gothenburg, Sweden. The façade, which has never been renovated, already shows signs of freeze-thaw degradation unevenly distributed along the façade surface. This indicates that the service life is exceeded on some parts of the building façade, see Figure 1.

Figure 2 shows the closest surroundings of the building. The investigated façade is facing south and is inclined 6 degrees to the west. The surrounding buildings are of the same height as the building of interest, shielding the façade from nearly all sides, with the closest building located 14.5 m in front of the façade. The exception is a free space which opens towards the southwest.

3.1. Input variables and model pre-requisites

The microclimate modelling is performed for 104 computational cells distributed over the façade surface. Two validated climate scenarios (A1B and A2) projecting hourly weather data for Gothenburg, Sweden, from 1961 to 2100 are used as input data for the analysis. Projected climate data are preferred over measured ones due to its completeness.

A modified version of an accurate 3D model of the building and its surroundings [13] is utilized in Rhino-Ladybug to obtain incident solar and long-wave radiation at the centre of each cell. Roofs including overhangs were manually added in accordance with the technical documentation of the buildings. The meshing process of the façade was conducted automatically in Rhino, assuming a cell to be approximately 1 m^2.

For the analysis, three computational cells are selected based on the preliminary estimation of solar radiation over the façade and over the course of all years. The cells represent areas on the façade with the highest (Cell A), average (Cell B) and the lowest (Cell C) incidence of solar radiation. Figure 3 depicts the exact position of the selected cells.

In this study, the wind-driven rain coefficients are calculated using the semi-empirical method from Straube and Burnett (SB) [14]. This method does not take the surroundings into account. Computational Fluid Dynamics (CFD) simulations can be used as well to obtain more exact wind-driven rain coefficients, reflecting the complexity of the surroundings. However, CFD simulation is not within the scope of this study. Therefore, the SB method is utilized instead. Figure 4 shows the definition of the Rain Admittance Factor (RAF) which is used within the SB method to differentiate wind-driven rain across a façade. RAF values for Cell A and Cell C are assumed equal (RAF = 1.0) to capture the effects of other input variables than wind-driven rain. Cell B has the RAF = 0.3.

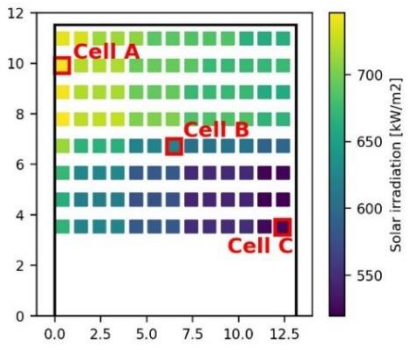

Figure 3. *Solar radiation over the façade averaged over the years 1961 - 2100*

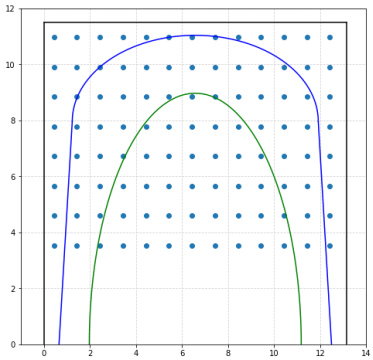

Figure 4. *Rain Admittance Factor (RAF) for the façade. Blue contour RAF =0.9, green contour RAF = 0.5.*

The boundary conditions for each cell obtained in the microclimate modelling are then used in the one-dimensional model in WUFI 2D-3. According to the technical documentation, the building

envelope consists of two layers. The inner layer is aerated concrete, and the outer layer is aerated bricks with a thickness of 200 mm and 108 mm, respectively. As the exact material parameters are not known, generic data from the WUFI material database is used. "Aerated concrete (600 kg/m^3) - old style" and "Aerated clay brick (675 kg/m^3)" materials are selected for the analysis. Additionally, material parameters for the bricklayer which are required for the FTDR assessment are taken from Zhou [12]. Solar absorptivity of 0.36 (-) for cream/glazed brick was chosen. The adhering fraction of rain was assumed to be 0.7. The indoor environment was modelled based on EN 15026 [3].

As mentioned above, the FTDR index is evaluated 2 cm below the outer surface, see Figure 5.

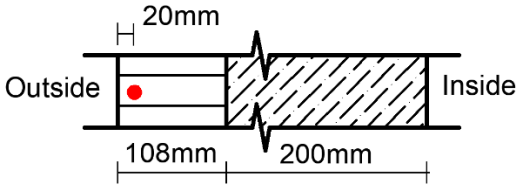

***Figure 5**. Sketch of the examined building envelope. The red dot represents an evaluation point for the FTDR index*

4. Results and discussion

The focus of this study is to assess the severity of freeze-thaw exposure of a brick façade and the difference before and after 2050. Furthermore, the severity of the MRYs is evaluated by hygrothermal modelling. The difference is also quantified for the different parts of the façade by simulating the degradation with boundary conditions based on the microclimate.

Figure 6 shows the results of the FDEI index and its two derivatives for the period between 1961 and 2100 and climate scenarios A1B and A2. Note that the results are normalized based on Eq. 3, i.e., to the maximum and minimum index values. The results show a decreasing freeze-thaw exposure in future climate scenarios across all indices. However, scenario A2 gives a steeper decline compared to the A1B scenario. Despite the similarities in the trend between the two indices, the more comprehensive indices mostly tend to estimate the severity of individual years differently as opposed to the basic FDEI index. Predominantly, this is due to the influence of the façade orientation and thus wind-driven rain as graphs for $FDEI_{WDR}$ and $FDEI_{WDR+solar}$ indices display only minor differences (see A.2 and A.3, B.2 and B.3).

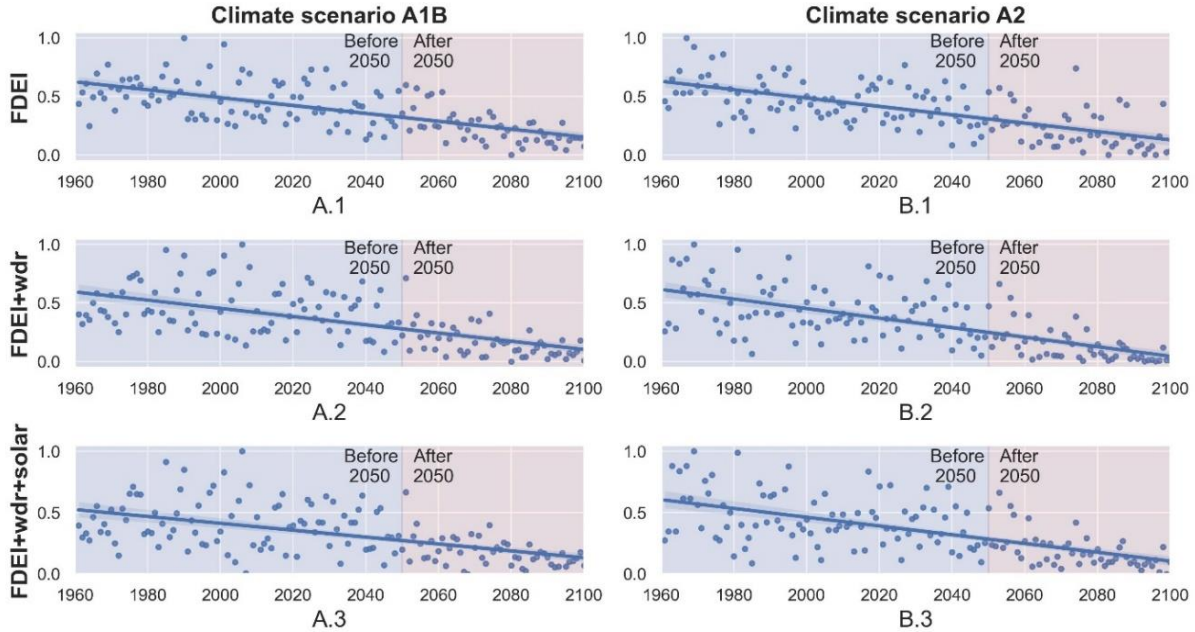

***Figure 6**. Fitted scatter plots of freeze-thaw exposure severity in Gothenburg, Sweden, for climate scenarios A1B (on the left) and A2 (on the right) throughout the years 1960 and 2100.*

Table 1 shows the resulting reference years for all examined indices, for years before and after 2050, and for scenarios A1B and A2, respectively. In general, reference years in all cases and for the whole examined period are always before the year 2050. Compared to that, reference years for the period after 2050 are lower by 29 to 34%.

Table 1. *MRY for two modified and unmodified FDEI indices and for the period before and after 2050, climate scenarios A1B and A2.*

	Prior 2050		*After 2050*			
	Scen. A1B	Scen. A2	Scen. A1B	Value norm.	Scen. A2	Value norm.
FDEI	1990	1967	2051	0.6	2074	0.74
$FDEI_{WDR}$	2006	1969	2051	0.71	2053	0.66
$FDEI_{WDR+solar}$	2006	1969	2054	0.66	2053	0.66

For the hygrothermal analysis and the indices evaluation, reference years as defined by $FDEI_{WDR+solar}$ are chosen - 2006 and 2054 for scenario A1B, and 1969 and 2053 for scenario A2. The reference years are applied on three different cells, each representing a different part of the façade as defined earlier (see Figure 3). In total twelve hygrothermal models are investigated. Two key points apply to the further investigation: 1) hygrothermal performance is assessed 2 cm below the outer surface (Figure 5), and 2) the results presented represent a quasi-steady state. The latter means that the reference year was used as a boundary condition for three consecutive years only the last year was selected for investigation. Figure 7 shows an example of such results.

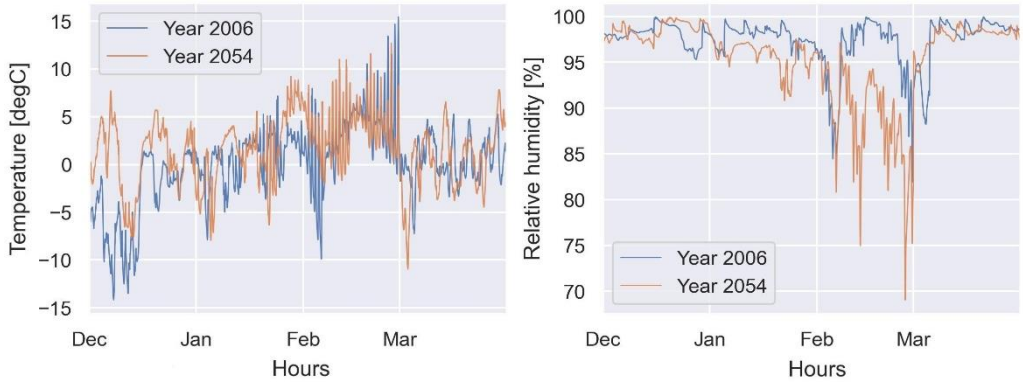

Figure 7*. Results of hygrothermal modelling 2 cm below the outside surface for Cell B and MRYs (i.e., 2006 and 2054) within the climate scenario A12. Results show only the winter period from December to the end of March.*

As Figure 7 shows, the winter period temperature 2 cm below the outside surface is lower in the year 2006 compared to 2054. Consequently, the relative humidity is higher in 2006 than in 2054. Both influencing parameters thus suggest the former year to be more critical. Indeed, this is further confirmed by the FTDR index evaluation in both climate scenarios and each cell. As Table 2 and Table 3 for climate scenarios A1B and A2 respectively show, the risk of degradation (FTDR index) drops between the examined years (i.e., from 21.26% to 44.28%).

***Table 2**. Results of FTDR and FDEI indices for the selected computational cells and selected reference years under the climate scenario A1B*

	FTDR					
	Cell A	Cell B	Cell C	$FDEI_{WDR+solar}$	FDEI	$FDEI_{WDR}$
Year 2006	16.74	7.38	16.91	1.00	0.73	1.00
Year 2054	13.17	5.77	11.47	0.66	0.57	0.40
Difference	21.26%	21.80%	32.17%	34.00%	21.92%	60.00%

***Table 3**. Results of FTDR and FDEI indices for the selected computational cells and selected reference years under the climate scenario A2*

	FTDR					
	Cell A	Cell B	Cell C	$FDEI_{WDR+solar}$	FDEI	$FDEI_{WDR}$
Year 1969	14.66	4.02	14.30	1.00	0.92	1.00
Year 2053	9.18	2.24	9.60	0.66	0.57	0.66
Difference	37.38%	44.28%	32.87%	34.00%	38.04%	34.00%

Further scrutiny of the FTDR index shows a considerably lower risk of degradation in the cell B compared to the other cells (i.e., 64% drop on average). This is due to the microclimate-based estimation of wind-driven rain, which is the lowest out of the three cells.

Small differences were also observed between cells A and C. Even though they are equally defined in terms of RAF coefficient (RAF = 1.0 in both), the wind-driven rain in each cell is different due to wind speed being defined differently for different heights. Furthermore, this also influences the convective heat transfer coefficients of the cells. Additionally, solar radiation and long-wave radiation are defined differently. As a result, the discrepancies in the FTDR indices are caused by the combination of these factors. The impact of these variables on the result is unknown at this point.

Interestingly, the differences between FTDR indices for the investigated years do not exhibit the same trend. The risk of degradation for the year 2006 is higher in cell C than in cell A as shown in Table 2. However, the opposite is found for the year 2054. Similar results were also found for climate scenario A2 in Table 3. These findings thus emphasize the complexity of the problem and the need for further research to better understand the dynamics of freeze-thaw degradation over building façades. This was also found in the case study façade where the degree of degradation varies over the façade.

To determine its effectiveness for MRY selection, the FDEI indices were compared to the FTDR indices by checking whether the ratio between the examined years is similar in both indices. As seen in Table 2, the FDEI indices overestimated their predictions compared to the FTDR index for scenario A1B. The average difference of the FTDR index is 25.08% while the $FDEI_{WDR+solar}$ differed by 34% (8.92% deviation) and the $FDEI_{WDR}$ index estimates the difference to be 60% (34.92% deviation). The basic FDEI index was closer to the FTDR with a 21.92% difference (-3.16% deviation). However, for scenario A2, the more comprehensive FDEI indices underestimated their predictions compared to the basic FDEI index, see Table 3. Both indices estimated the difference to be 34% which is below the average FTDR difference (38.17%) by 4.17%. The basic FDEI index differed by 38.04% deviating only by 0.13%.

5. Conclusion

This study aimed to investigate the severity of freeze-thaw degradation in brick buildings in Gothenburg, Sweden, in the future compared to the present. The differences in degradation risks over

the façade surface were also investigated. This was done by hygrothermal modelling of a façade using reference years as a base for microclimate modelling.

The first finding of this study was that the FDEI index is more accurate than its derivatives ($FDEI_{WDR}$ and $FDEI_{WDR+solar}$ index). This was shown by proportionally comparing results for the FDEI indices with the risk of freeze-thaw degradation quantified by the FTDR index for different MRY. Furthermore, the risk of freeze-thaw degradation in Gothenburg, Sweden is decreasing for the location of the façade after 2050. Finally, there is a difference in the risk of freeze-thaw degradation by 64% on average between the compared parts on the façade. The main contribution to this difference is the definition of the wind-driven rain coefficient. Consequently, the differences caused by the examined MRYs do not show the same difference. This is due to the higher solar radiation not always resulting in a lower risk of degradation. Finally, this study shows the importance of carefully choosing the most suitable boundary conditions for façade modelling, ideally using CFD modelling. In future research, guidelines for practitioners on how to best model the service life will be developed.

References

[1] "ByggaF-metoden | Fuktcentrum." shorturl.at/syQRV / (accessed Jan. 16, 2023), Lund, Sweden
[2] Zhou X, Carmeliet J, and Derome D, "Assessment of risk of freeze-thaw damage in internally insulated masonry in a changing climate," *Build. Environ.*, vol. 175, p. 106773, May 2020, doi: 10.1016/j.buildenv.2020.106773.
[3] "SS-EN 15026:2007 Hygrothermal performance of building components and building elements – Assessment of moisture transfer by numerical simulation." Brussels, Belgium.
[4] Vandemeulebroucke I and Caluwaerts S, "Review and Evaluation of 20 Methods to Select Moisture Reference Years for Damage Risks in Solid Masonry Walls," presented at the 2022 *Thermal Performance of the Exterior Envelopes of Whole Buildings XV International Conference*, 2022, December 5-8, Clearwater Beach, Florida
[5] Grossi C M , Brimblecombe P, and Harris I, "Predicting long term freeze–thaw risks on Europe built heritage and archaeological sites in a changing climate," *Sci. Total Environ.*, vol. 377, no. 2, pp. 273–281, May 2007, doi: 10.1016/j.scitotenv.2007.02.014.
[6] "ISO 15927-3:2009 Hygrothermal performance of buildings - Calculation and presentation of climatic data - Part 3: Calculation of a driving rain index for vertical surfaces from hourly wind and rain data," Technical Standard ICS: 07.060; 91.120.10, 2009, Geneva, Switzerland.
[7] Lisø K R, Kvande T, Hygen H O, Thue J V, and Harstveit K, "A frost decay exposure index for porous, mineral building materials," *Build. Environ.*, vol. 42, no. 10, pp. 3547–3555, Oct. 2007, doi: 10.1016/j.buildenv.2006.10.022.
[8] Mandinec J, Johansson P, and A. S. Kalagasidis, "Full facade exposure to freeze-thaw degradation," *Build. Environ.* [to be submitted]
[9] Sadeghipour Roudsari M, Pak M, Viola A, "Ladybug: A Parametric Environmental Plugin For Grasshopper To Help Designers Create An Environmentally-conscious Design," presented at the 2013 Building Simulation Conference, August 26-28, Chambéry, France. doi: 10.26868/25222708.2013.2499.
[10] "WUFI® 2D | WUFI (en)." https://wufi.de/en/software/wufi-2d/ (accessed Jan. 19, 2023), Holzkirchen, Germany
[11] Trindade A D, Coelho G B A, and Henriques F M A, "Influence of the climatic conditions on the hygrothermal performance of autoclaved aerated concrete masonry walls," *J. Build. Eng.*, vol. 33, p. 101578, Jan. 2021, doi: 10.1016/j.jobe.2020.101578.
[12] Zhou X, Derome D, Carmeliet J, "Hygrothermal modeling and evaluation of freeze-thaw damage risk of masonry walls retrofitted with internal insulation," *Build. Environ.*, vol. 125, pp. 285–298, Nov. 2017, doi: 10.1016/j.buildenv.2017.08.001.
[13] Logg A, Naserentin V, and Wästberg D, "DTCC Builder." Digital Twin Cities Centre, 2022
[14] Straube J F and Burnett E E P, "Simplified prediction of driving rain deposition," *Int. Build. Phys. Conf.*, Eidhoven, September 12-21, 2000, pp. 375–382.